**Supplementary Fig. 1 Ex vivo staining with anti-CD45RC MAb on rat cells.** Gating strategy of CD45RC analysis on cell subset from PBMCs from rats. Cells were first gated on morphology, excluding doublets cells and DAPI+ dead cells. Representative experiment of 6.
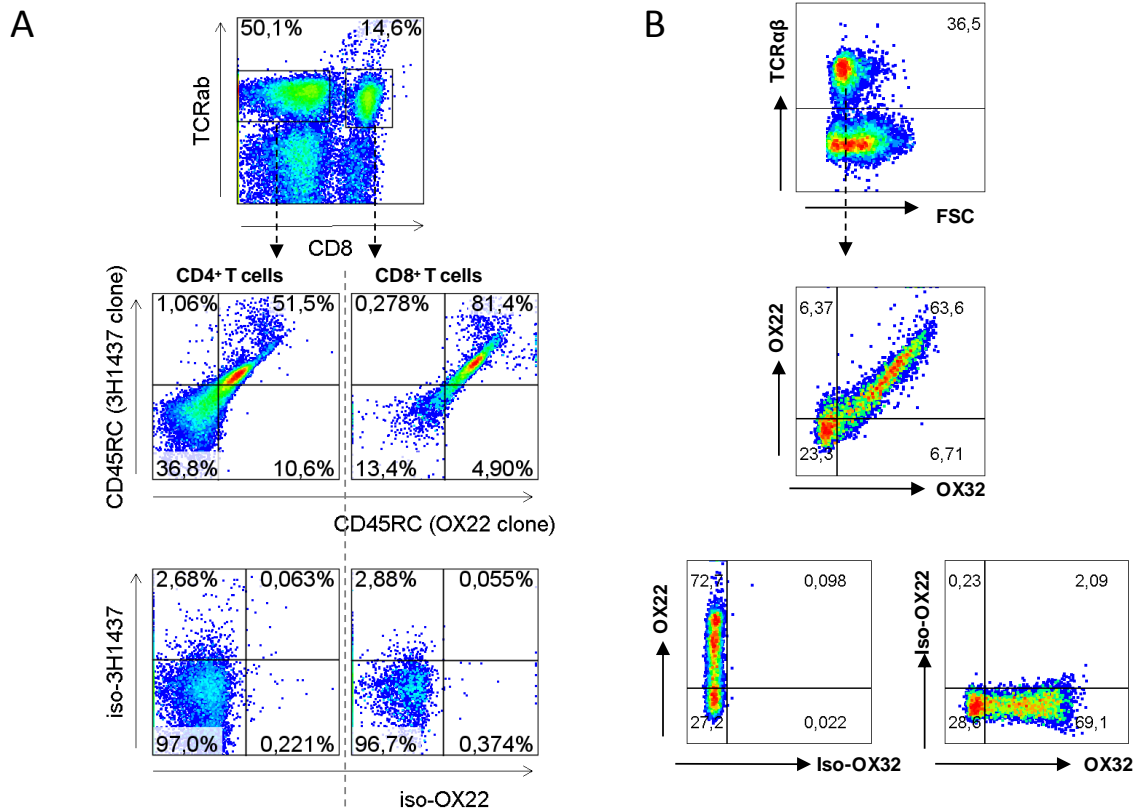
Supplementary Fig. 2 Flow cytometry staining using distinct anti-CD45RC MAbs for CD45RC^{+} cells tracking. PBMCs were recovered from naive animals and analyzed for CD45RC staining using three distinct Abs recognizing a different epitope, OX22, OX32 and 3H1437 clones. Cells were gated on living CD4^{+} or CD8^{+} T cells for OX22 and 3H1437 staining (**A**) or living T cells for OX22 and OX32 staining (**B**), stained successively and analyzed by flow cytometry. A representative experiment of 2 individuals.
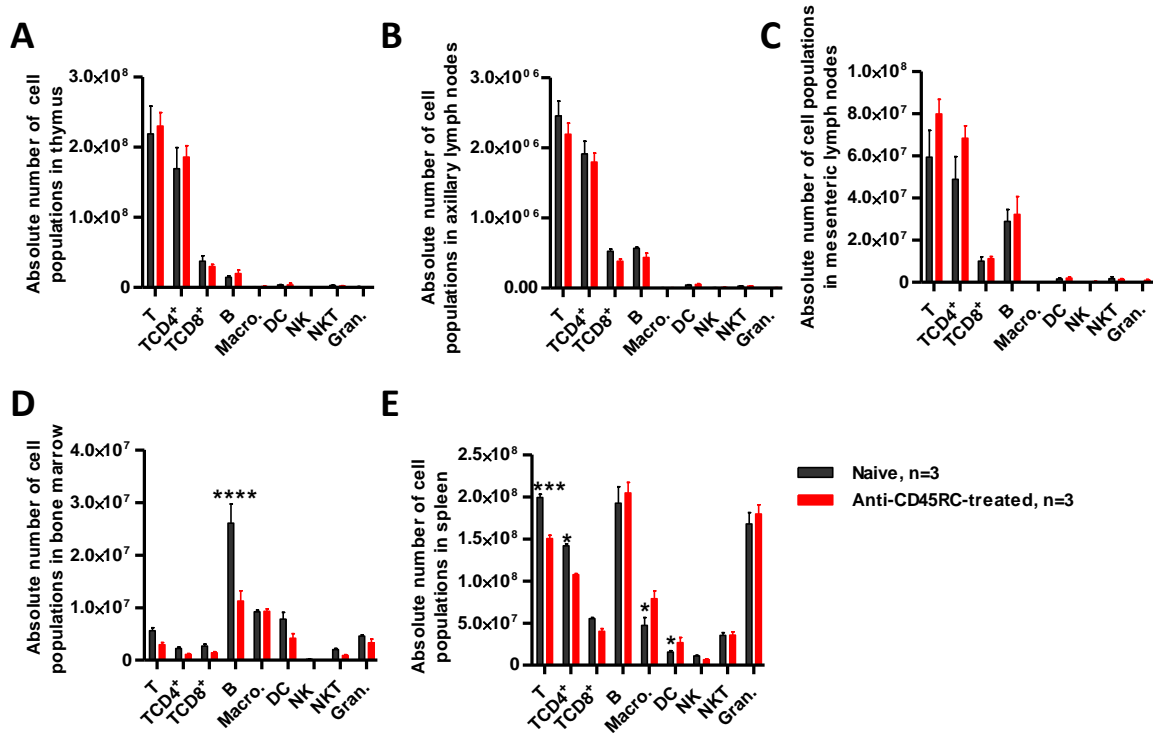
Supplementary Fig. 3 Short-term anti-CD45RC treatment resulted in minimal modification of leucocytes composition in non-blood compartments of long term tolerant recipients. (**A**) Thymus, (**B**) Mesenteric and (**C**) axillary lymph nodes, (**D**) bone marrow, and (**E**) spleen were analyzed for cell subsets composition (T cells, B cells, macrophages, DCs, NK cells, NKT cells and granulocytes) 120 days after transplantation and anti-CD45RC treatment, and compared with naive rats. n=3 for all groups. Friedman test, Dunn's post test. *p<0.05; ***p<0.001; ****p<0.0001.
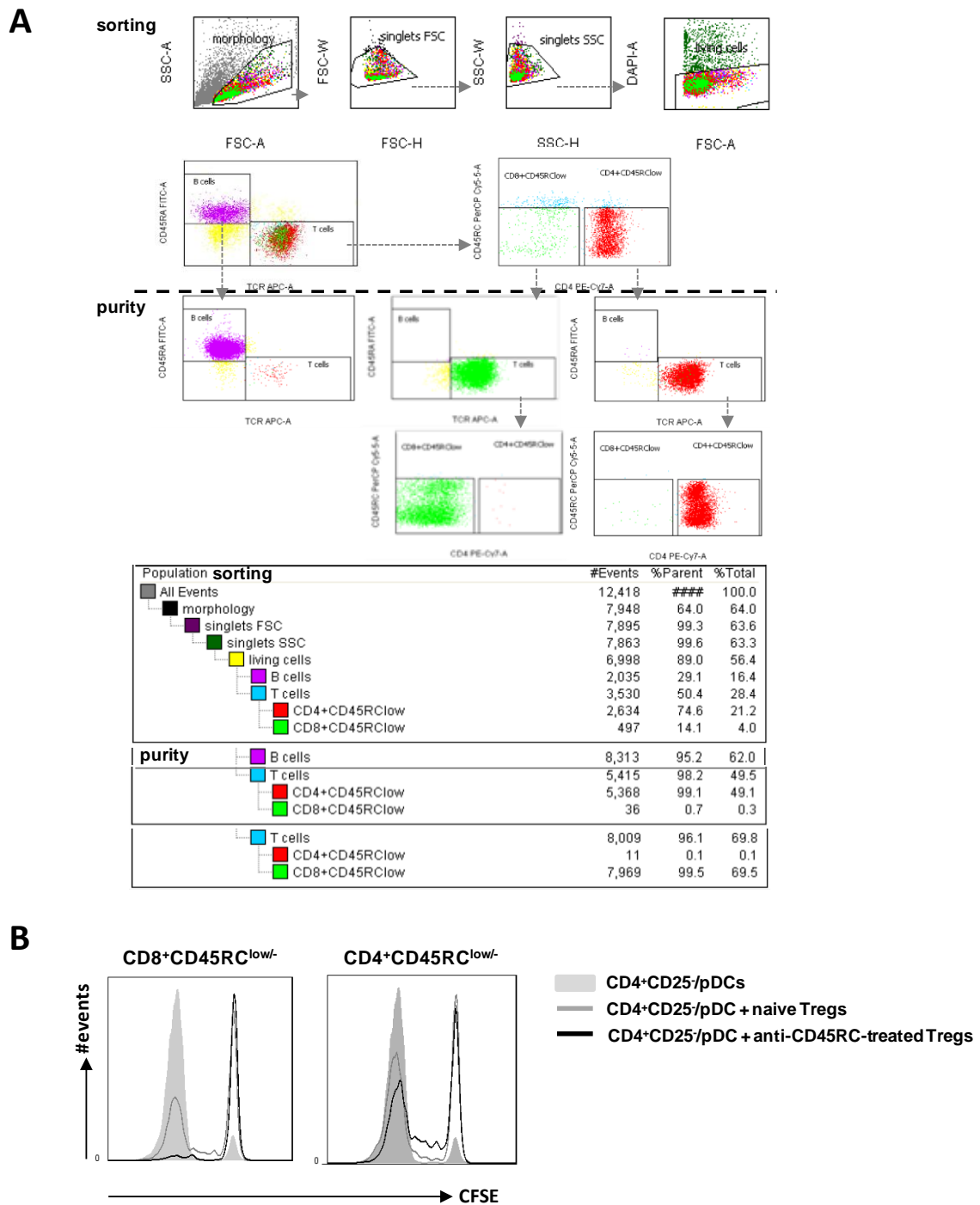
A

B

C

D
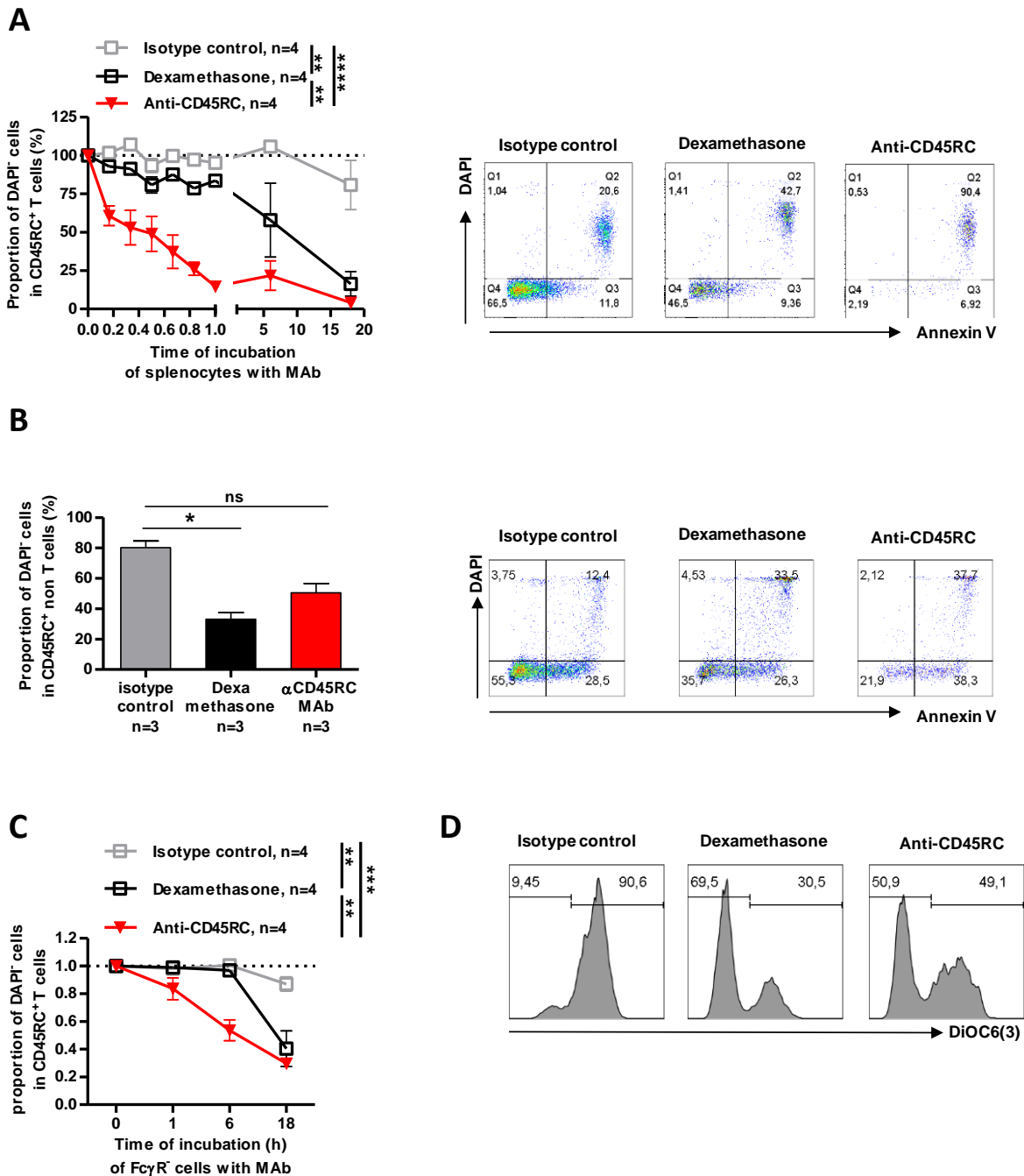
Supplementary Fig. 4 Efficient apoptosis induction following CD45RC targeting critically contributes to tolerance induction to cardiac allograft in rat. Total splenocytes were incubated with anti-CD45RC MAb or isotypic controls in presence of heat-inactivated rat serum (i.e. absence of complement). Dexamethasone was used as positive controls. CD45RC$^+$ T cells for 10 min to 18h **(A)** or non-T cells for 18h **(B)** were analyzed by flow cytometry for DAPI labeling. Right : representative experiment at 1h. A: Two Way ANOVA

RM test. **$p<0.01$, ****$p<0.0001$. B: Friedman and Dunn's post test *$p<0.05$. **(C)** Splenocytes depleted from FcγR^+ cells were incubated with anti-CD45RC MAb or isotype control in presence of heat-inactivated frozen rat serum for 10 min to 18h. Dexamethasone was used as positive controls. CD45RC^+ T cells were analyzed by flow cytometry for DAPI labeling. Two Way ANOVA RM test. **$p<0.01$, ***$p<0.001$. **(A-C)** Results are expressed as relative proportion of positive cells among CD45RC^+ T cells ± SEM. n=4 for all groups. **(D)** Total splenocytes were incubated with anti-CD45RC MAb or isotypic controls in presence of heat-inactivated frozen rat serum for 1 to 18h. Dexamethasone was used as positive controls. CD45RC^+ T cells were analyzed by flow cytometry for DiOC6(3) labeling. One representative experiment. Two Way ANOVA RM test. **$p<0.01$, ***$p<0.001$.

A

| Population **sorting**	#Events	%Parent	%Total
All Events	12,418	####	100.0
morphology	7,948	64.0	64.0
singlets FSC	7,895	99.3	63.6
singlets SSC	7,863	99.6	63.3
living cells	6,998	89.0	56.4
B cells	2,035	29.1	16.4
T cells	3,530	50.4	28.4
CD4+CD45RClow	2,634	74.6	21.2
CD8+CD45RClow	497	14.1	4.0
purity B cells	8,313	95.2	62.0
T cells	5,415	98.2	49.5
CD4+CD45RClow	5,368	99.1	49.1
CD8+CD45RClow	36	0.7	0.3
T cells	8,009	96.1	69.8
CD4+CD45RClow	11	0.1	0.1
CD8+CD45RClow	7,969	99.5	69.5

B

CD8+CD45RClow/-   CD4+CD45RClow/-

- CD4+CD25-/pDCs
- CD4+CD25-/pDC + naive Tregs
- CD4+CD25-/pDC + anti-CD45RC-treated Tregs

Supplementary Fig. 5 CD8+ and CD4+CD45RClow/- T cells were assessed for suppressive activity in ex vivo culture assays and for in vivo adoptive transfers. (A) Gating strategy and purity of FACS Aria cell sorting of B cells and CD4+CD45RClow and CD8+CD45RClow T cells from anti-CD45RC treated rats. Purity was greater than 95%. Representative experiment. **(B)** Representative histograms of 3 experiment of suppressive assay where CFSE-labeled

LeW.1A CD4$^+$CD25$^-$ T cells were stimulated with allogeneic LEW.1W pDCs in absence (filled light grey) or presence of CD8$^+$CD45RC$^{low/-}$ (left) or CD4$^+$CD45RC$^{low/-}$ (right) Tregs from LEW.1A anti-CD45RC-treated long-term tolerant recipients (black line) or naive rats (grey line) at ratio effector : suppressor 1:1. Proliferation was analyzed by gating on DAPI$^-$ CPD450$^-$CD4$^+$T cells after 6 days of culture.

A

B
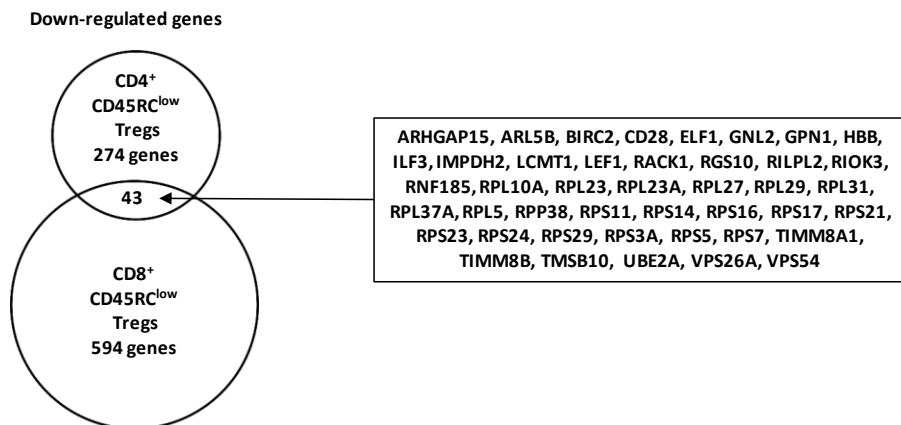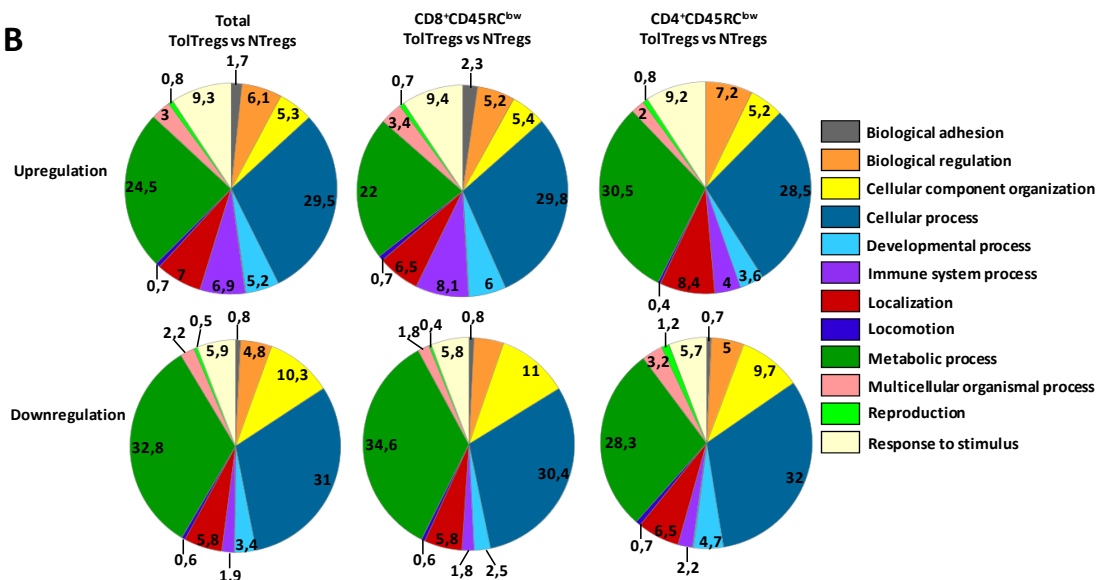
Supplementary Fig. 6 RNA sequencing of Tregs from anti-CD45RC treated tolerant recipient as compared to natural Tregs. (A) Venn diagrams were drawn based on downregulated genes from RNA-seq data sets. Circles depict unique and shared genes downregulated by $CD4^+$ and $CD8^+$ $CD45RC^{low}$ Tregs from anti-CD45RC MAb treated vs untreated rats. The squares represent a subset of the list of downregulated genes corresponding to each part of the circles. (B) PANTHER gene ontology analysis of functional annotations associated with upregulated or downregulated genes unique or shared by $CD4^+$ and $CD8^+$ $CD45RC^{low}$ Tregs from CD45RC MAb treated vs untreated rats. Each color represents different functions. Results are expressed in percentage of modified genes expression.

A

B
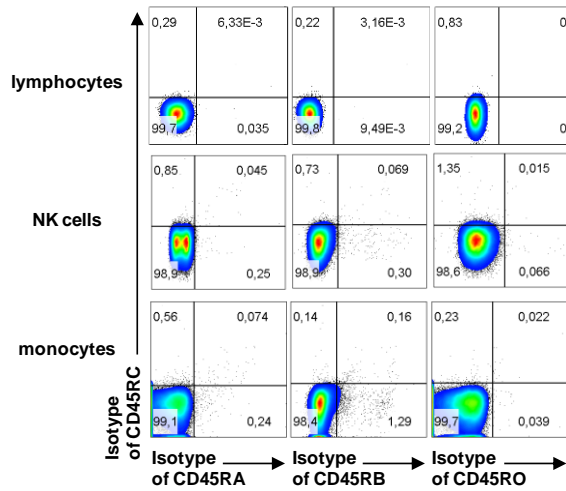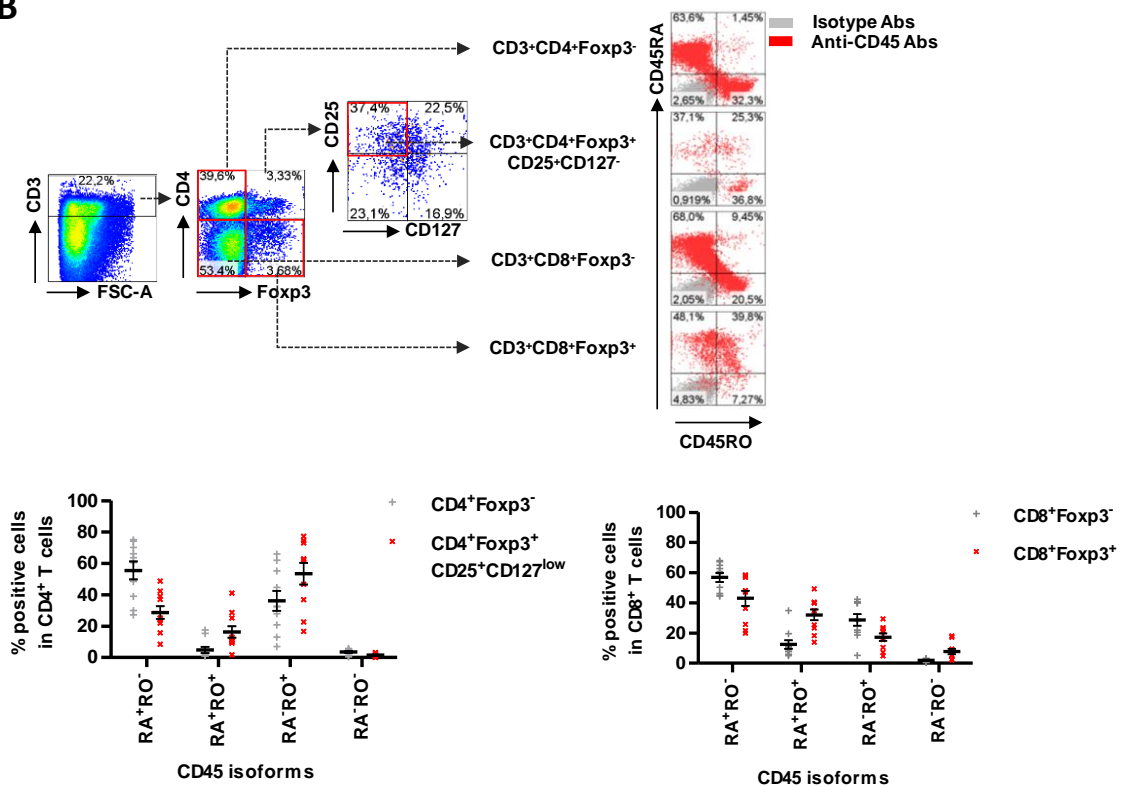
Supplementary Fig. 7 Flow cytometry staining with CD45 isoforms isotype matched controls MAbs. (A) Lymphocytes, NK cells and monocytes were analyzed for isotype control staining by flow cytometry. Representative experiment of 10 individuals. **(B)** Co-expression pattern analysis of CD45RA and CD45RO on CD4^{+} and CD8^{+} subsets among T cells. A representative dot plot analysis of 10 healthy volunteers and mean+/-SEM of

CD45RA and CD45RO positive cells among $CD4^+CD25^+CD127^-$ Tregs, $CD8^+Foxp3^+$ Tregs, $Foxp3^-CD4^+$ and $Foxp3^-CD8^+$ T cells.
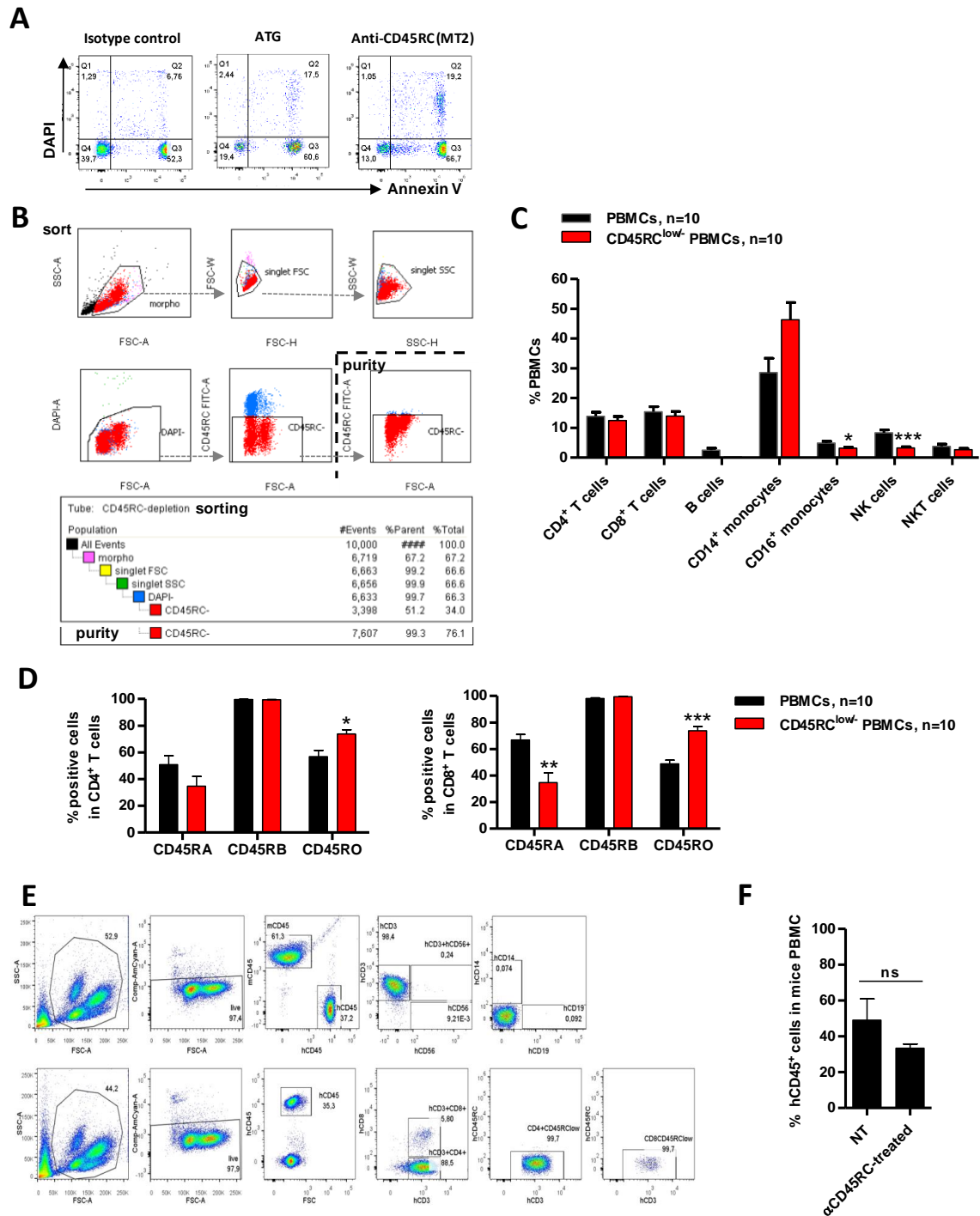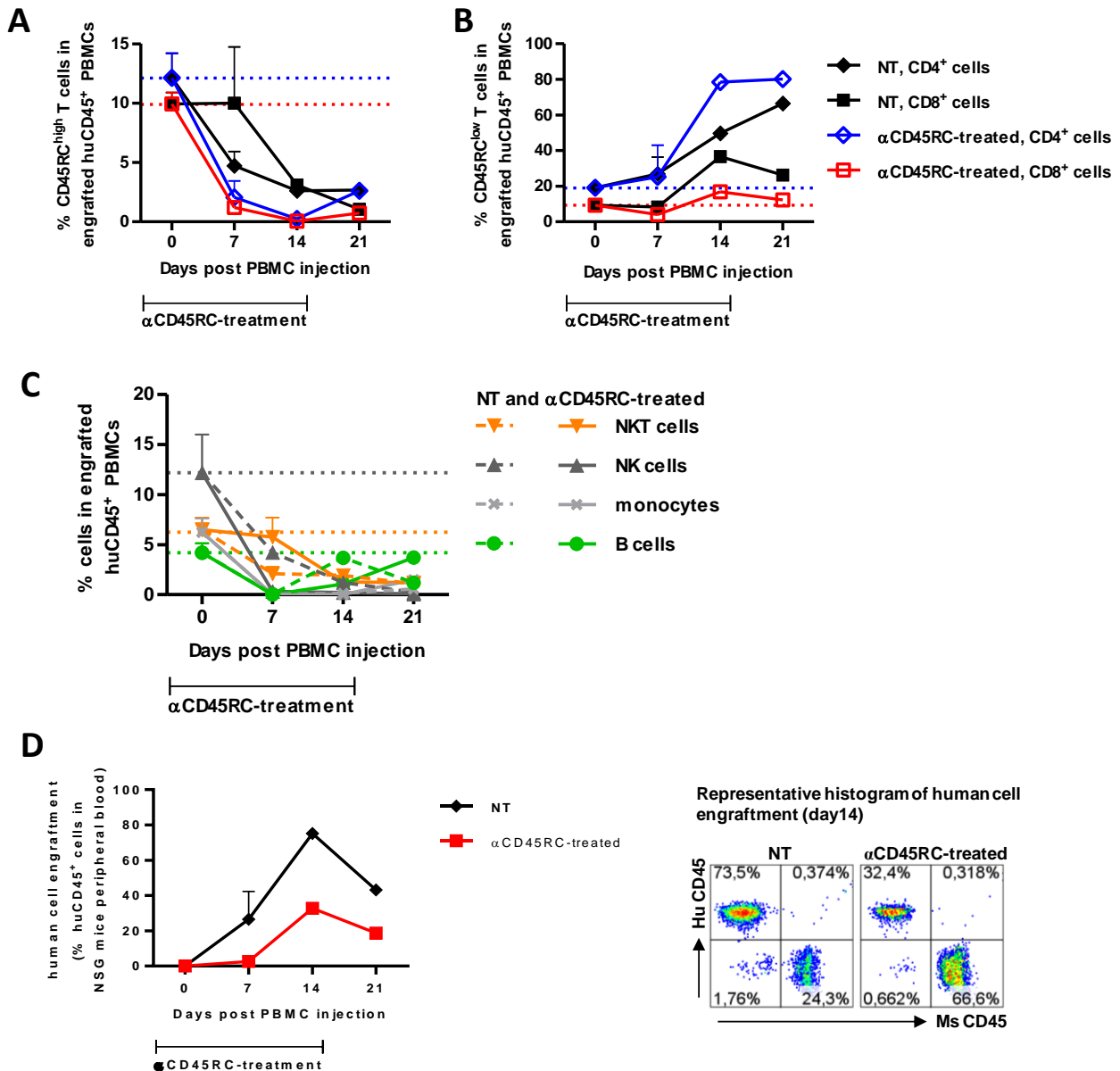
Supplementary Fig. 8. In vitro and in vivo assessment of anti-CD45RC MAb treatment on human cells. (A). PBMCs from healthy human volunteers were incubated with anti-CD45RC (MT2 clone), isotype control (mouse IgG1), or ATG and analyzed for DAPI/Annexin V staining in CD3$^+$ cells. Representative experiment of 3. **(B)** Gating strategy and purity of FACS Aria cell sorting of CD45RC negative PBMCs from healthy volunteers

for adoptive transfer. Purity was greater than 99%. Representative experiment of 6. Proportion of immune cells remaining following cell sorting among total PBMCs **(C)** and proportion of isoforms of CD45 **(D)** in 10 healthy volunteers**.** **(E)** Representative staining of 3 mice. **(F)** Long surviving mice injected with CD45RC-depleted PBMCs were analyzed for human CD45$^+$ cell engraftment in mice blood.

Supplementary Fig. 9 In vivo assessment of anti-CD45RC MAb treatment on human cells. Mice injected with anti-CD45RC MAb or not and human PBMCs were analyzed for the percentage of CD45RC^{high} **(A)** and CD45RC^{low} **(B)** T cells; NKT, NK, B cells or monocytes **(C)** in engrafted huCD45$^+$ PBMCs; and for total human CD45$^+$ cell engraftment in mice blood **(D)**. Results are expressed as mean+/-SEM of cell proportion in human PBMCs **(A-C)** or mice blood cells **(D)**.